J Mol Model (2013) 19:951–961
DOI 10.1007/s00894-012-1639-1

ORIGINAL PAPER

Regioselectivity in Sonogashira synthesis of 6-(4-nitrobenzyl)-2-phenylthiazolo[3,2-b]1,2,4-triazole: a quantum chemistry study

Tayebeh Hosseinnejad · Majid M. Heravi · Rohoullah Firouzi

Received: 27 February 2012 / Accepted: 7 October 2012 / Published online: 25 October 2012

Abstract In the present research, the experimentally observed regioselectivity in Sonogashira synthesis of 6-(4-nitrobenzyl)-2-phenylthiazolo[3,2-b]1,2,4triazole has been modeled by means of density functional theory (DFT) employed to investigate the structural and thermochemical aspects of this synthesis in the gas and solution phases. Comparison of our calculated structural parameters of the title compound with the available X-ray crystallographical data demonstrate a reliable agreement. Then, the effect of two different solvents, DMF and ethanol, are examined via polarized continuum model calculations, showing a significant decrease in the computed values of the reaction enthalpy and free energy changes compared with the gas phase results. We have also considered two tautomeric structures of the intermediate species that it seems the mode of its intermolecular cyclization has an important role in regioselectivity of the final products. Moreover, all obtained results in the gas and solution phases also confirm that the synthesis of the title compound is thermodynamically more favorable than the other regioisomeric product. We also discuss the thermodynamical feasibility of this reaction at higher temperatures. Finally, we concentrate on the survey of substituent effect by choosing electron-withdrawing and electron-donating groups on the aryl iodide. Our calculated thermochemical data in the gas and solution phases indicate that the use of electron-withdrawing moieties is more favorable thermodynamically than electron-donating ones which has been previously concluded via the experimental elucidations.

Keywords Density functional theory · Polarized continuum model · Regioselectivity · Sonogashira reaction · 1,2,4-triazoles

T. Hosseinnejad (✉) · M. M. Heravi
Department of Chemistry, Faculty of Science, Alzahra University, Vanak,
Tehran, Iran
e-mail: tayebeh.hosseinnejad@gmail.com

R. Firouzi
Chemistry & Chemical Engineering
Research Center of Iran (CCERCI),
P. O. Box 14335-186, Tehran, Iran

Introduction

The compounds derived from 1,2,4-triazoles have attracted significant research interests due to their widespread biological and pharmalogical activities specially as antifungal drugs [1–4]. Although many efforts have been devoted to the preparation of 1,2,4-triazoles by palladium catalyzed annulations strategies [5–7], the recent work of Heravi et al. [8] have led to a regioisomeric substituted thiazolo [3,2-b]1,2,4-triazoles with high yield and good regioselectivity during Sonogashira coupling reaction.

Among the variety of palladium-catalyzed coupling methods [9–13], Sonogashira coupling reaction [13–16] of aryl halides with terminal acetylenes provides an effective route for C-C bond formation which has been recently reviewed by Heravi [17]. This name reaction has become a useful method for the preparation of aryl alkynes and conjugated enynes, having been widely applied as a key step in the bioactive substance synthesis [3, 4].

In the aforementioned work of Heravi et al. [8], 5-phenyl-3-propargylmercapto-1,2,4-triazole **1** was first treated with 4-nitro-1-iodobenzene **2** to afford 5-phenyl-3-[4-nitro propargylmercapto phenyl]1,2,4-triazole as intermediate species via Sonogashira cross-coupling reaction catalyzed by bis (triphenylphosphine) palladium chloride. In the next step, the intermediate species was followed by its corresponding end product via a palladium catalyzed intermolecular cyclization process and the major product of this synthesis was

characterized as 6-(4-nitrobenzyl)-2-phenylthiazolo[3,2-b] 1,2,4-triazole **3** with yield of 81 % which was accompanied by another regioisomeric product **4** displayed schematically in Fig. 1.

The X-ray crystallographical data have identified and provided explanations in favor of formation of **3** while other spectral data were not significantly helpful in this contest. It should be mentioned that Heravi and coworkers have also reported the regioselective synthesis of other 1,2,4-triazole derivatives in many experimental papers and discussed the origin of the occurred regioselectivity [18–20]. They have discussed that depending on the mode of intermolecular cyclization, two regioisomeric products can be obtained and concluded that due to α-effect the nitrogen2 of 1,2,4-triazole is more reactive than the nitrogen4 leading to produce a regioisomer with more yield than the other. They have proved and supported this behavior with experimental data and the X-ray structural elucidations.

From the computational viewpoint, accurate information on the energetics for this synthesis can be one of the important aspects of addressing the regioselectivity challenge that could be due to either thermodynamic or kinetic effects. It should be stated that in ref. [8] Heravi and coworkers have suggested a two-step mechanistic pathway for this synthesis that includes a standard Sonogashira coupling followed by a Pd(II)-catalyzed intermolecular cyclization. Aside from this traditional mechanism, they predicted two alternative plausible mechanisms for this reaction. The computational study

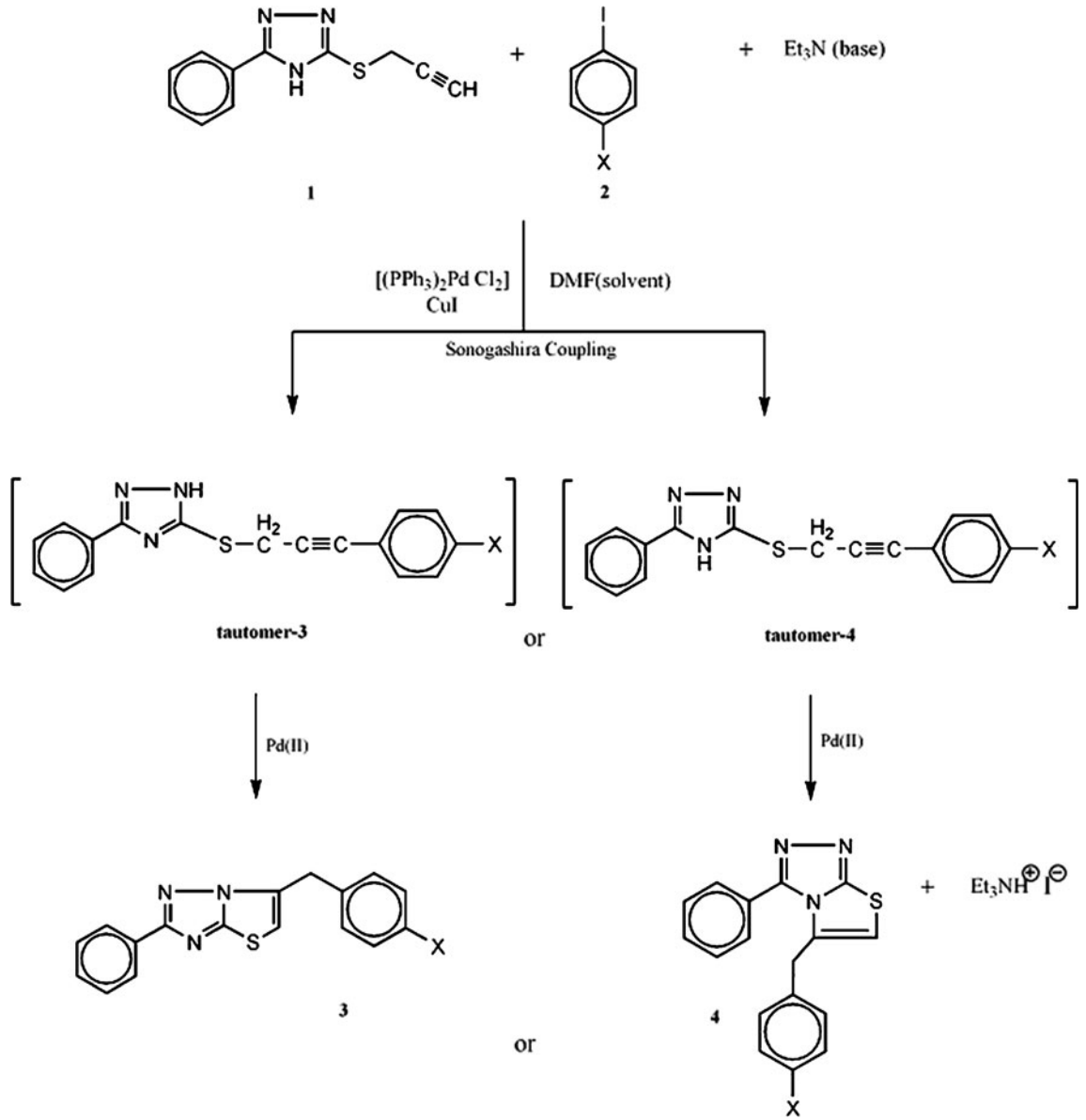

Fig. 1 Schematic diagram of Sonogashira cross-coupling reaction investigated in this work. The labels of reactants, intermediate and products were identified in the main text

of full catalytic Sonogashira pathway for this synthesis is under way.

The main objective of this study is to computationally investigate the underlying reasons for the experimentally observed regioselectivity in Sonogashira synthesis of 6-(4-nitrobenzyl)-2-phenylthiazolo[3,2-b]1,2,4-triazole **3** [8] from the structural and thermodynamic viewpoints. In this context, we have only focused on the quantum chemical evaluation of the changes in thermodynamic properties of this reaction (see Fig. 1) based on density functional theory (DFT) [21, 22]. We first determine the structural features of **3** in the gas phase and dimethylformamide (DMF) solution at two levels of DFT calculations, followed by comparing the calculated results with the available X-ray crystallogarphical data (reported in ref. [8]). These comparisons show that our obtained optimized geometry can well reproduce the crystal structure parameters of **3** while two DFT methods have the near accuracy in prediction of geometry.

We then asses the polarized continuum model (PCM) [23] to analyze the effect of various chemical environments on the reaction energies. Strictly speaking, we compute the free energy and enthalpy changes of the reaction in the presence of DMF as a polar and aprotic solvent in order to investigate its thermodynamical preference in comparison with ethanol medium as a protic solvent with lower polarity. It is important to note that in many experimental studies [17, 24], aprotic solvents have been widely preferred for the reactions that contain strong bases such as Sonogashira cross-coupling synthesis. Another significant aspect of this work is the evaluation of temperature effect in thermochemistry of the reaction that leads to a considerable change in the reaction Gibbs free energies.

The results reported in the experimental work of ref.[8], imply that the presence of electron-withdrawing groups on the aryl iodide is essential in the product yield and regioselectivity while the use of PhI leads to a complicated regioisomeric mixture. Therefore, we finally focused on the substituent effect in this synthesis via DFT calculations. To this end, we computationally investigate the effect of some electron-withdrawing and electron-donating substituents in terms of the reaction electronic energies and thermochemical properties in the gas and solution phases. The results are in agreement with the thermodynamic preference of using electron-withdrawing groups to achieve a higher yield and more regioselective synthesis, as has already been noticed experimentally [8].

Computational details

We have carried out the DFT computational study of the aforementioned Sonogashira coupling reaction (displayed in Fig. 1) by determining the ground state structures of all reagents, intermediates and products without any symmetry restrictions in the geometry optimization procedure. We then utilized harmonic frequency analysis to confirm that the found optimized geometries correspond to the true minima. We also employed the vibrational frequencies to obtain enthalpies and Gibbs free energies in temperatures, 298, 400 and 500 K. The calculation of energetics as well as geometry optimizations was performed at two levels of DFT methods to assess the performance of these methods in prediction of geometry and energy: i) 6-31G* using the popular B3LYP level of theory which consists of a hybrid Becke-Hartree-Fock exchange and a Lee-Yang-Parr correlation functional with nonlocal corrections [22] and ii) 6-311 +G* basis set with M06 functional which has been introduced recently as a hybrid meta-GGA (generalized gradient approximation) exchange-correlation functional that was parametrized including both transition metals and nonmetals

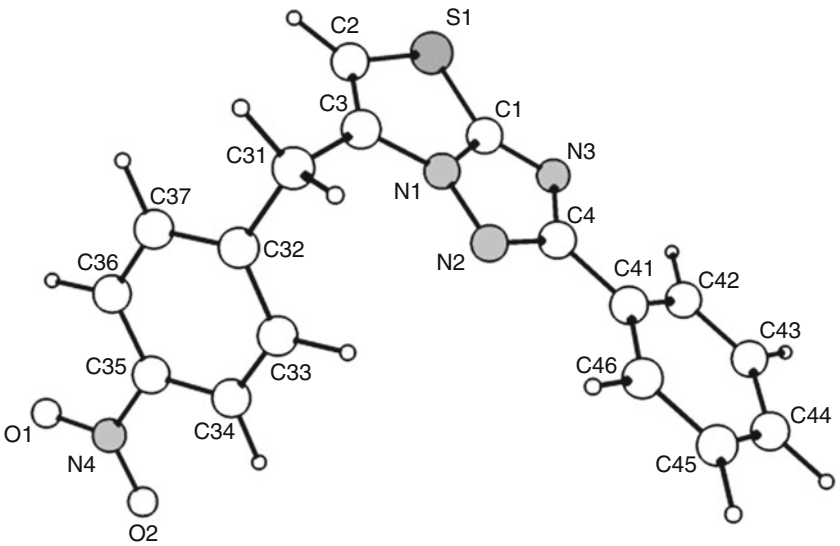

Fig. 2 The optimized geometry of compound 3, calculated at M06/6-311+G* level of theory

Table 1 The selected bond lengths and angles of compound **3**, calculated at M06/6-311+G* level of theory in the gas and solution phases together with X-ray values. Two last columns contain the deviation percents between the calculated results (in gas and solution phases) with crystallographical data. The corresponding values of these bond lengths and angles calculated at B3LYP/6-31G* level of theory have been given in parenthesis

Bond lengths (Å)	Calculated M06/6-311+G* (B3LYP/6-31*)		Experimental (X-ray)	Dev (%)	
	Gas phase	Solution phase		Gas phase	Solution phase
S1-C1	1.735(1.743)	1.728(1.741)	1.722	−0.754(−1.257)	−0.393(−1.107)
S1-C2	1.759(1.770)	1.757(1.770)	1.745	−0.802(−1.463)	−0.710(−1.436)
C2-C3	1.348(1.356)	1.349(1.355)	1.345	−0.223(−0.820)	−0.361(−0.774)
N1-C1	1.357(1.364)	1.352(1.361)	1.352	−0.369(−0.896)	−0.069(−0.692)
N1-C3	1.384(1.392)	1.390(1.396)	1.396	0.859(0.214)	0.742(0.194)
N1-N2	1.347(1.358)	1.350(1.358)	1.361	1.028(0.250)	0.427(−0.007)
C4-N2	1.334(1.342)	1.333(1.342)	1.337	0.224(−0.415)	0.261(−0.382)
N3-C4	1.366(1.375)	1.367(1.374)	1.372	0.437(−0.230)	0.345(−0.187)
N3-C1	1.309(1.317)	1.313(1.321)	1.319	0.758(0.144)	0.435(−0.225)
C3-C31	1.490(1.505)	1.489(1.505)	1.494	0.267(−0.759)	0.323(−0.769)
C4-C41	1.461(1.468)	1.464(1.470)	1.471	0.679(0.149)	0.471(0.040)
C35-N4	1.475(1.471)	1.465(1.462)	1.465	−0.682(−0.429)	−0.010(0.163)
N4-O1	1.213(1.231)	1.217(1.233)	1.226	1.060(−0.416)	0.685(−0.646)
N4-O2	1.213(1.230)	1.217(1.233)	1.226	1.060(−0.378)	0.709(−0.648)
Bond angles (°)					
C1-S1-C2	89.150(89.136)	88.985(89.125)	89.67	0.579(0.595)	0.763(0.607)
S1-C2-C3	113.813(113.813)	114.004(113.835)	114.0	0.164(0.164)	−0.003(0.144)
C2-C3-N1	110.004(109.864)	109.674(109.785)	109.5	−0.460(−0.332)	−0.158(−0.260)
C3-N1-N2	117.002(117.351)	117.144(117.114)	116.4	−0.517(−0.817)	−0.693(−0.614)
N1-N2-C4	101.658(101.781)	101.785(101.895)	101.1	−0.551(−0.673)	−0.677(−0.786)
N2-C4-N3	115.569(115.355)	115.395(115.280)	116.1	0.457(0.641)	0.607(0.706)
C4-N3-C1	101.945(102.063)	101.962(102.062)	101.5	−0.438(−0.554)	−0.455(−0.553)
N3-C1-S1	138.495(138.431)	137.858(138.336)	138.2	−0.213(−0.167)	0.247(−0.098)
N3-C1-N1	110.947(111.045)	111.008(110.945)	111.2	0.227(0.139)	0.172(0.229)
N1-C3-C31	120.451(120.911)	120.903(121.224)	120.0	−0.375(−0.759)	−0.752(−1.020)
C3-C31-C32	111.532(113.777)	111.421(113.433)	112.1	0.506(−1.495)	0.605(−1.189)
C35-N4-O2	117.523(117.743)	118.144(118.276)	118.2	0.572(0.386)	0.047(−0.064)

and was recommended for application in organometallic and inorganometallic thermochemistry, kinetic studies and non-covalent interactions [25]. In the case of iodine, the relativistic effective core potential (RECP) determined by Hay-Wadt [26], LANL2DZ, with accompanying basis set was used.

We have then estimated the solvent effects on the structure and thermodynamic features of the aforementioned Sonogashira synthesis (see Fig. 1) via PCM method based on a continuum representation of the solvent surrounding the substances [23]. All DFT calculations have been performed using GAMESS suite of programs [27].

Table 2 Thermochemistry of the reaction calculated at M06/6-311+G* and B3LYP/6-31G* levels of theory in the gas phase. ΔE_e is the reaction energy from the total electronic energies, ΔE_0 is the reaction energy with zero-point energies included. ΔH, ΔG and ΔS are the reaction enthalpy, free energy and entropy change, respectively. Note that the conversion energy change values are in kcal mol^{-1} and the entropy change values are in cal/mol.K

Regioselective isomer	M06/6-311+G*					B3LYP/6-31G*				
	ΔE_e	ΔE_0	ΔH	ΔG	ΔS	ΔE_e	ΔE_0	ΔH	ΔG	ΔS
Isomer **3**	34.65	41.24	42.67	50.37	−25.83	28.47	35.46	41.45	49.79	−27.98
Isomer **4**	46.08	52.49	53.55	63.46	−33.25	44.19	50.61	56.07	64.43	−28.05

Results and discussion

The primary objective of this research is to assess the ability of quantum chemistry computations to predict the geometry of **3** via comparing with the available X-ray crystal structure [8].

In this respect, we have first determined the optimized structure of **3** at B3LYP/6-31G* and M06/6-311+G* levels of theory by performing geometry optimization procedure in the gas phase and also PCM method with DMF as the solvent. The theoretical optimized structure of **3** obtained at M06/6-311+G* level of theory in the gas phase together with the atomic numbering are presented in Fig. 2. Some of M06/6-311+G* calculated bond lengths and angles of **3** in the gas and DMF solution phases as well as X-ray ones are summarized in Table 1. We have also presented the corresponding values of these bond lengths and angles calculated at B3LYP/6-31G* level of theory in parenthesis. Importantly, Table 1 includes the deviation percents between our calculated results and crystallographical data.

The average absolute deviation (AAD) of X-ray experimental data with M06/6-311+G* calculated values in the gas and solution phases are 0.54 % and 0.42 %, respectively. More precisely, the maximum absolute deviation of M06/6-311+G* calculated bond lengths and angles in the gas phase with the experimental ones are 1.06 % (0.68 %) and 0.57 % (0.76 %) correspond to R(N4-O1) and A(C1-S1-C2), respectively. Note that the values within brackets are the maximum absolute deviation of the X-ray data with the calculated results in the solution phase. Moreover, the AAD of X-ray data with B3LYP/6-31G* calculated ones in the gas and solution phases are 0.55 % and 0.52 %, respectively. This means that these two levels of theory have near accuracy to reproduce the X-ray structure of compound **3**.

As was mentioned earlier, assessment of the reaction environment effect in estimation of the reaction energetic is a challenging task in theoretical calculations. Therefore, we first discuss the calculated reaction energy and thermodynamic properties changes in the gas phase, followed by analyzing the effect of DMF and ethanol as aprotic and protic solvents, respectively.

The calculated thermochemical data, including reaction energies (with and without zero-point energy corrections), enthalpies, Gibbs free energies and entropies computed at B3LYP/6-31G* and M06/6-311+G* levels of theory in the gas and two solution phases are presented in Table 2 and 3, respectively. The following three facts can be deduced from the stringent analysis of the reported results in Tables 2 and 3: i) the production of **3** in the gas and solution phases should be more favorable thermodynamically than **4** in the synthesis. ii) by a comparative survey in the obtained results at two levels of theory, it seems that the employment of larger basis set and more modern functional leads to a

Table 3 Thermochemistry of the reaction calculated at M06/6-311+G* level of theory with the presence of DMF and ethanol as solvents via PCM method. The definitions of ΔE_e, ΔH, ΔG and ΔS quantities are the same as Table 2. The corresponding values of the aforementioned properties calculated at B3LYP/6-31G* level of theory have been given in parenthesis. Note that the conversion energy change values are in kcal mol^{-1} and the entropy change values are in cal/mol.K

Regioselective isomer	DMF solvent				Ethanol solvent			
	ΔE_e	ΔH	ΔG	ΔS	ΔE_e	ΔH	ΔG	ΔS
Isomer **3**	−69.59(−79.38)	−57.37(−67.07)	−49.66(−59.68)	−25.87(−24.79)	−68.15(−77.89)	−55.54(−65.56)	−48.22(−58.15)	−24.56(−24.86)
Isomer **4**	−62.79(−67.82)	−51.10(−56.30)	−41.80(−49.02)	−31.20(−24.42)	−61.25(−66.26)	−48.57(−54.70)	−40.27(−47.24)	−27.85(−25.03)

decrease of about 4 kcal mol^{-1} in the difference between the reaction energies of regioisomer **3** and **4** both in the gas phase and solution. However, we discussed earlier the close accuracy of these two levels of theory for the prediction of geometry iii) the calculated values of reaction enthalpy changes demonstrate the high endothermicity of the synthesis in the gas phase while inclusion of solvent effects leads to an exothermic synthesis. This behavior can be attributed mainly to the high dissociation energy of triethylammonium iodide which is stabilized significantly due to solvent effects in comparison with the gas phase conditions.

The computed Gibbs free energy values demonstrate that the thermodynamic feature of this synthesis is quantitatively different from the calculated reaction enthalpy changes due to the entropic effects. Indeed, the calculated Gibbs free energy changes of the reaction become more positive than those obtained for enthalpy changes values with increasing of around 8 kcal mol^{-1} in the gas and solution phases that could be assigned to the negative values of the reaction entropy change which is around −0.025 kcal mol^{-1}.K at 298 K. The B3LYP/6-31G* and M06/6-311+G* calculated values of the reaction entropy changes have been reported in Tables 2 and 3 for the gas and two solution phases.

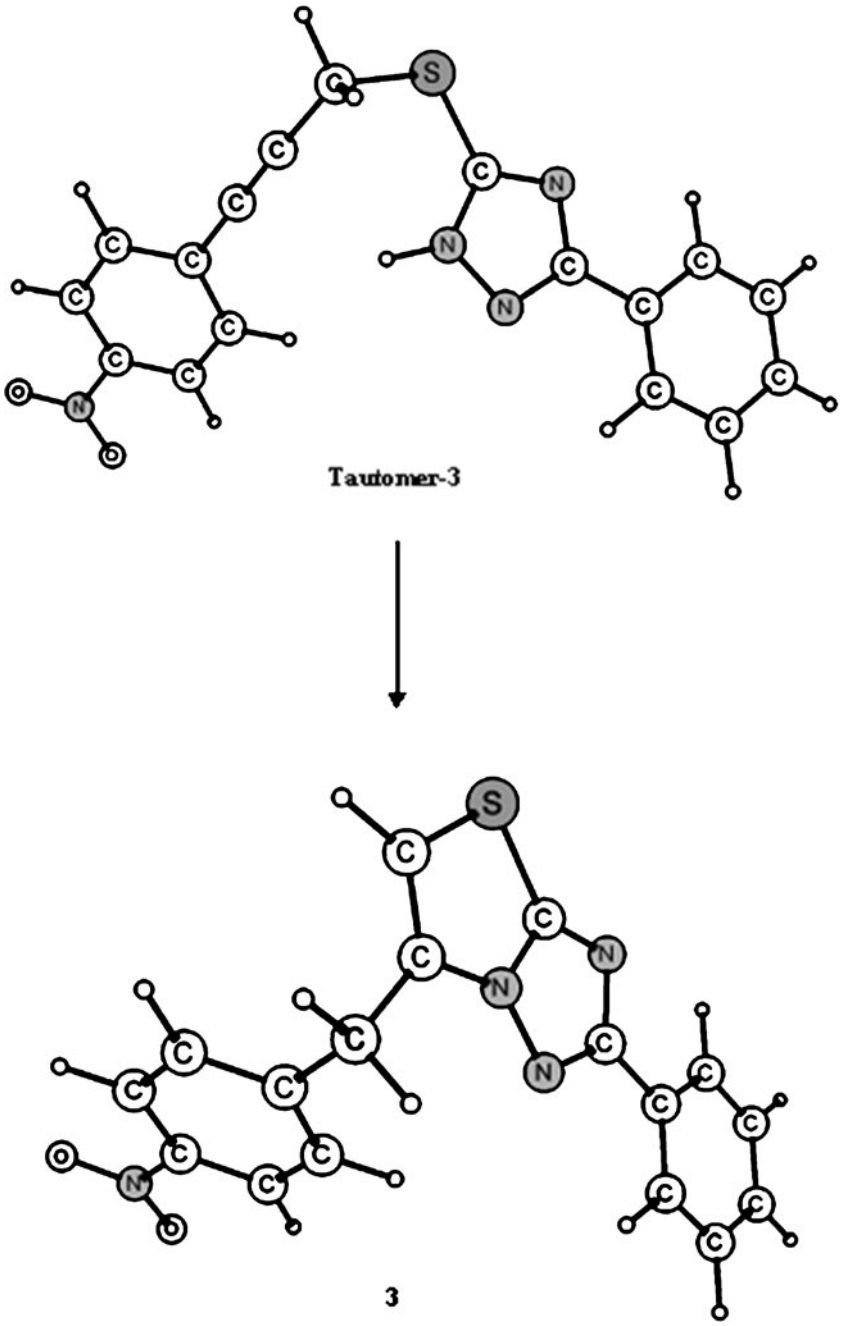

Fig. 3 The theoretical M06/6-311+G* optimized geometries of tautomer-3 and its corresponding regioisomeric product **3**

Another notable discussion that can be concluded from the calculated results of Table 3 is the preference of using aprotic solvents in comparison with protic ones in the Sonogashira synthesis. The computed values of reaction enthalpy changes suggest that employing DMF as aprotic solvent with dielectric constant, $\varepsilon=38$, and dipole moment, $\mu=3.82$ D, is thermodynamically more favorable than ethanol as protic solvent with dielectric constant, $\varepsilon=30$, and dipole

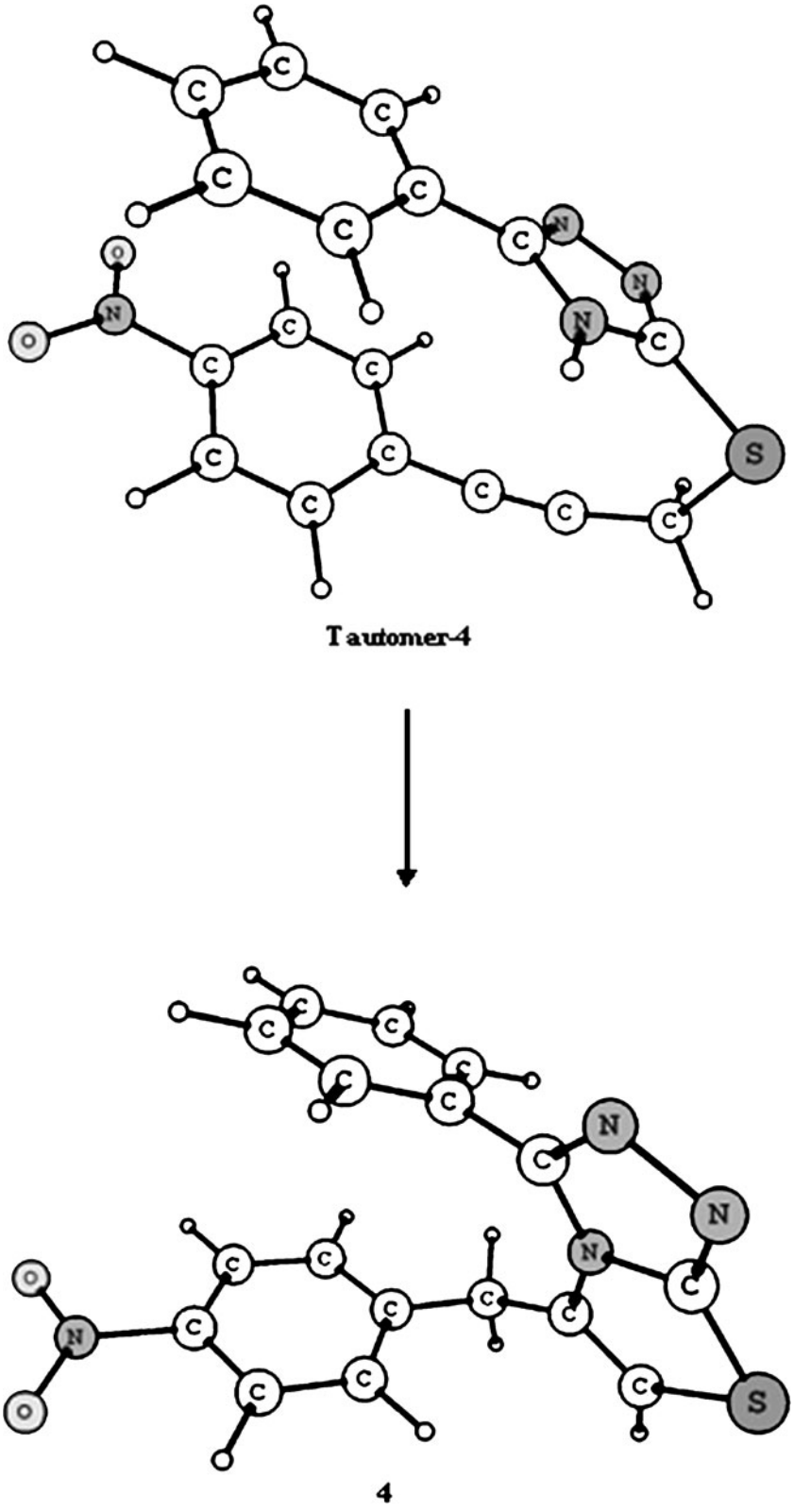

Fig. 4 The theoretical M06/6-311+G* optimized geometries of tautomer-4 and its corresponding regioisomeric product **4**

Table 4 Electronic energy of two tautomers of intermediate (expressed as $E_{e,t}$). The electronic energy, enthalpy, Gibbs free energy and entropy changes for the conversion of each tautomeric intermediate to its corresponding regioisomeric product (denoted as $\Delta E_{e,t-p}$, ΔH_{t-p}, ΔG_{t-p} and ΔS_{t-p}, respectively). Note that the electronic energies have reported in hartree, the conversion energy change values are in kcal mol^{-1} and the entropy change values are in cal/mol.K

	Gas phase					Solution phase				
	$E_{e,t}$	$\Delta E_{e,t-p}$	ΔH_{t-p}	ΔG_{t-p}	ΔS_{t-p}	$E_{e,t}$	$\Delta E_{e,t-p}$	ΔH_{t-p}	ΔG_{t-p}	ΔS_{t-p}
Tautomer-3	−1422.0703	−33.05	−30.99	−27.01	−13.35	−1422.0895	−31.22	−29.17	−25.18	−13.38
Tautomer-4	−1422.0674	−23.43	−22.64	−21.01	−5.46	−1422.0887	−24.93	−24.13	−23.11	−3.42

moment, μ=1.69 D. It is worthwhile to note that the difference between our obtained values of the reaction energy and thermochemical properties changes for DMF and ethanol PCM calculations is around 2 kcal mol^{-1}. This means that the different behavior of protic and aprotic solvents could not be clearly distinguished by thermodynamic computations. Thus, we anticipate that this issue to be described more distinctly in the kinetic studies.

In the next step, we confined our attention to another significant feature of this synthesis that it seems has a major role in the observed regioselectivity. As was mentioned earlier, based on the mode of intermolecular cyclization in 5-phenyl-3-[4-nitro propargylmercapto phenyl]1,2,4-triazole as intermediate species, two regioisomeric final products were generated that can be mainly attributed to the two tautomeric structures of intermediate. Hence, we investigated computationally the structure and energetics of two suggested tautomers of intermediate species. The theoretical optimized geometries of each tautomers of intermediate (entitled as tautomer-3 and tautomer-4) and their corresponding regioisomeric product have been represented in Figs. 3 and 4, respectively. In Table 4, we have reported M06/6-311+G* calculated

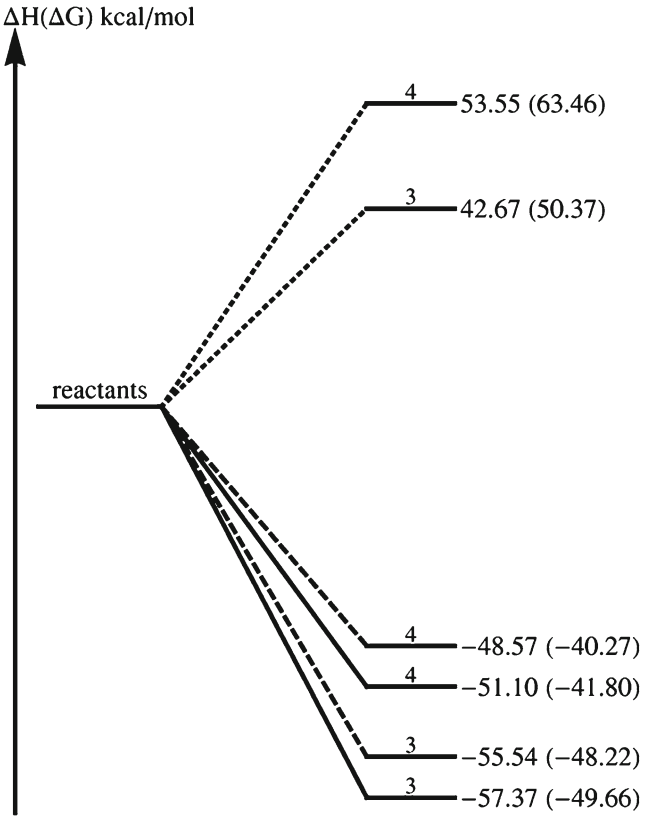

Fig. 5 A comparative illustration for the enthalpy changes during the regioselective synthesis displayed in Fig. 1, calculated at M06/6-311+G* level of theory in the gas phase (dotted line ….) and with the presence of ethanol (dashed line —) and DMF (solid line) as solvents by inclusion of solvation model. The corresponding values of the reaction Gibbs free energy changes have been given in parenthesis. All energy values are relative to the reactants

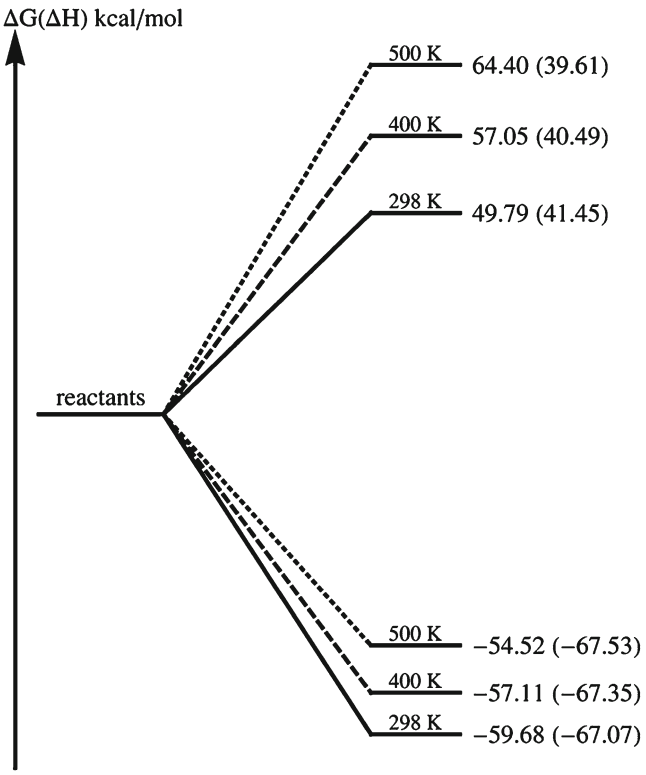

Fig. 6 Schematic of Gibbs free energy changes during the reaction represented in Fig. 1, calculated in the gas and solution phases at three temperatures: 298 K (solid line), 400 K (dashed line —) and 500 K dotted line ….). The corresponding values of the enthalpy changes have been given in parenthesis. All energy values are relative to the reactants

Table 5 Thermochemistry (in kcal mol^{-1}) of the reaction calculated at B3LYP/6-31G* level of theory in the gas phase with the presence of various substituents on aryl iodide. X denotes the substituted group on para position of ArI. ΔE_e, ΔE_0, ΔH and ΔG are defined same as Table 2

ArI X	Isomer **3**				Isomer **4**			
	ΔE_e	ΔE_0	ΔH	ΔG	ΔE_e	ΔE_0	ΔH	ΔG
H	29.55	36.49	42.44	50.34	45.05	51.39	56.78	64.89
NO_2	23.77	30.58	36.96	43.72	39.16	46.03	52.43	60.02
CN	28.47	35.46	41.45	49.79	44.19	50.61	56.07	64.43
OCH_3	29.51	36.12	41.78	49.55	44.96	51.41	56.88	65.45

values of the electronic energies for two tautomers of intermediate in the gas and solution phases together with the enthalpy, Gibbs free energy and entropy changes for the conversion of each tautomers of intermediate to its corresponding regioisomeric product. Based on the results of Table 4, we could claim that the conversion of tautomer-3 to its corresponding final product **3** is more favorable thermodynamically than the conversion of tautomer-4 to the regioisomeric product **4** while this step of the synthesis is exothermic in the gas and solution phases.

Another interesting aspect can be analyzed from the comparison of our reported results in Tables 2 and 3 with Table 4. As is clear from the reported results of Table 2 and 3, the difference between enthalpy changes for generating regioisomeric products **3** and **4** is about 10 kcal mol^{-1} that means only the regioisomer **3** should be observed in the experiment. Despite this relatively large difference, the enthalpy change for the conversion of tautomer-3 to its corresponding end product **3** is about 7 kcal mol^{-1} less than the enthalpy change for the conversion of tautomer-4 to its corresponding end product **4**. Furthermore, the difference between electronic energies of two suggested tautomers of intermediate is about 0.0029 hartree (1.81 kcal mol^{-1}). These facts may partly confirm the presence of another regioisomeric end product **4** observed in the synthesis as a byproduct with yield of about 19 %.

Our calculated enthalpy changes of this synthesis together with the Gibbs free energy values at 298 K in the gas and two solution phases have been displayed in a schematic representation in Fig. 5.

To describe the effect of temperature on the enthalpy and Gibbs free energy changes of the reaction, we have carried out DFT assessment at higher reaction temperatures (400 and 500 K). A comparative illustration for the calculated enthalpy and Gibbs free energy changes at 298, 400 and 500 K has been shown in Fig. 6. As can be seen in Fig. 6 upon an increase in temperature, there is a small change in the calculated reaction enthalpies while the calculated reaction free energies increase considerably specially in the solution. In other words we predict that at higher temperatures, this synthesis would become less thermodynamically favorable in the gas and solution phases.

As was mentioned earlier, various experimental studies have proposed that the yield of products and regioselectivity in Sonogashira synthesis are influenced by the presence of electron-withdrawing and electron-donating groups on the aryl iodide [8, 28, 29]. The final goal of this work is therefore to computationally investigate this feature in terms of thermodynamic factors. For this investigation, NO_2 and CN species as electron-withdrawing groups and OCH_3 as electron-donating were considered to be on para position of PhI molecule. Then, we used DFT calculations to analyze the thermodynamic property changes of the reaction in the presence of aforementioned substituents in comparison with the absence of substituent on aryl iodide. The resulting properties in the gas and solution phases are listed in Tables 5 and 6, respectively. As is clear from Table 5, a slight decrease is observed in ΔE_e, ΔE_0, ΔH and ΔG calculated values for all substituents in the gas phase, while substitution of NO_2 on PhI seems to be more favorable thermodynamically. On the other hand, a similar theoretical outcome is obtained on the substituent effect from the solution phase calculations in the presence of DMF as solvent (given in Table 6).

From the thermochemical perspective, the reported results of Tables 5 and 6 clearly propose that i) compound **3** is more stabilized and consequently its production is more favorable than **4** and ii) the thermodynamic feasibility of the

Table 6 The same as Table 5, calculated in the solution phase at B3LYP/6-31G* level of theory via PCM method

ArI X	Isomer **3**				Isomer **4**			
	ΔE_e	ΔE_0	ΔH	ΔG	ΔE_e	ΔE_0	ΔH	ΔG
H	−77.82	−70.99	−65.09	−56.75	−66.22	−59.98	−54.59	−46.50
NO_2	−82.53	−76.39	−71.05	−63.09	−70.39	−63.99	−58.36	−50.37
CN	−79.38	−72.84	−67.07	−59.68	−67.82	−61.70	−56.30	−49.02
OCH_3	−77.76	−71.44	−65.90	−58.77	−66.25	−60.16	−54.82	−47.32

aforesaid synthesis is more favorable in the presence of electron-withdrawing moieties in comparison to the electron-donating ones. It is worthwhile to note that this behavior has been observed previously for this synthesis by consideration of product yields in the presence of various substituents [8].

A meticulous review of the results reported in Tables 5 and 6 shows that due to the proximity between the calculated thermochemical values with various substituents, it would also be useful to study this effect from the reaction mechanism point of view.

Conclusions

In this work, we presented a thermochemical study of Sonogashira synthesis of 6-(4-nitrobenzyl)-2-phenylthiazolo[3,2-b]1,2,4-triazole using two levels of DFT computational method. In the first step, the validation of our calculated structural properties of the title compound was represented by comparison with the available X-ray crystallographical data that demonstrated a reliable agreement. Our calculated reaction enthalpies and free energies in the gas and solution phases indicate three important facts: i) the production of compound **3** is thermodynamically more favorable than its regioisomer **4**. ii) The employment of larger basis set and more modern functional leads to a decrease of about 4 kcal mol^{-1} in the difference between the reaction energies of regioisomer **3** and **4** while there is a close accuracy between these two levels of theory for the prediction of geometry. iii) According to our computational results on the tautomeric structures of intermediate species, we have demonstrated that the intermolecular cyclization of tautomer-3 to generate its corresponding final product **3** is more favorable thermodynamically than the conversion of tautomer-4 to the regioisomeric product **4** that may be one of the main origins of regioselectivity.

We also demonstrated the preference of employing DMF (as an aprotic solvent) in comparison with ethanol (as a protic one) in this synthesis. Furthermore, according to our DFT computations in gas and solution phases at higher temperatures, this synthesis would become less favorable from the thermodynamic viewpoint.

A comparative study on the reaction thermochemical properties with various substituents on aryl iodide indicated that although inclusion of electron-withdrawing groups makes this synthesis more regioselective in favor of **3**, there is a small distinction between the calculated thermochemical values of the reaction with the different substituents. Therefore, we wish to suggest that kinetic factors should be considered to make a definite conclusion about the substitution effect. Finally, it should be emphasized that all our obtained thermochemical results including solvent, temperature and substituent effects considerations, are in reasonable agreement with the experimentally observed regioselectivity.

Acknowledgments The authors gratefully acknowledge the partial financial support received from the research council of Alzahra University. We have also thank to Prof. Mitra Ghassemzadeh for providing us X-ray crystallographical data. The first author is also grateful to Dr. M.H. Karimi-Jafari for his invaluable comments.

References

1. Erol DD, Calis U, Demirdamar R, Yully N, Ertan M (1995) Synthesis and biological activities of some 3,6-disubstituted thiazolo[3,2-b][1,2,4]triazoles. J Pharm Sci 84:462–465
2. Odds FC, Abbott AB (1984) Antifungal relative inhibition factors: BAY 1–9139, bifonazole, butoconazole, isoconazole, itraconazole (R 51211), oxiconazole, Ro 14-4767/002, sulconazole, terconazole and vibunazole (BAY n-7133) compared in vitro with nine established antifungal agents. J Antimicrob Chemother 14:105–114
3. Doucet H, Hierso JC (2007) Palladium-based catalytic systems for the synthesis of conjugated enynes by sonogashira reactions and related alkynylations. Angew Chem 46:834–871
4. Chinchilla R, Najera C (2007) The Sonogashira reaction: a booming methodology in synthetic organic chemistry. Chem Rev 107:874–922
5. Dale DJ, Cartwright BA, Clark AJ, Mc Naib H (2001) Gas-phase pyrolysis of 4-amino-3-allylthio-1,2,4-triazoles: a new route to [1,3]thiazolo[3,2-b][1,2,4] triazoles. J Chem Soc Perkin Trans 1:424–428
6. Katritzky AR, Pastor A, Varonkov M, Steel PJ (2000) Novel one-step synthesis of Thiazolo[3,2-b]1,2,4-triazoles. Org Lett 2:429–431
7. Kochhar MM, Williams A (1972) Bicyclic triazoles. 1.3-(2-Furyl)-5-phenylthiazolo-2,3-c)-s-triazole. J Med Chem 15:332–333
8. Heravi MM, Kivanloo A, Rahimzadeh M, Bakavoli M, Ghassemzadeh M, Neumüller B (2005) Regioselective synthesis of 6-benzylthiazolo[3,2-b]1,2,4-triazoles during Sonogashira coupling. Tetrahedron Lett 46:1607–1610
9. Heck RF, Nolley JP Jr (1972) Palladium-catalyzed vinylic hydrogen substitution reactions with aryl, benzyl, and styryl halides. J Org Chem 37:2320–2322
10. Milstein D, Stille JK (1978) A general, selective, and facile method for ketone synthesis from acid chlorides and organotin compounds catalyzed by palladium. J Am Chem Soc 100:3636–3638
11. Miyaura N, Suzuki A (1995) Palladium-catalyzed cross-coupling reactions of organoboron compounds. Chem Rev 95:2457–2483
12. Negishi E, Takahashi T, Babu S, Van Horn DE, Okukado N (1987) Palladium- or nickel-catalyzed reactions of alkenylmetals with unsaturated organic halides as a selective route to arylated alkenes and conjugated dienes: Scope, limitations, and mechanism. J Am Chem Soc 109:2393–2401
13. Sonogashira K, Tohda Y, Hagihara N (1975) A convenient synthesis of acetylenes: catalytic substitutions of acetylenic hydrogen with bromoalkenes, iodoarenes and bromopyridines. Tetrahedron Lett 16:4467–4470
14. Sonogashira K (2002) Development of Pd-Cu catalyzed cross-coupling of terminal acetylenes with s^{p2}-carbon halides. J Organomet Chem 653:46–49
15. Hassan J, Sévignon M, Gozzi C, Schulz E, Lemaire M (2002) Aryl-aryl bond formation one century after the discovery of the Ullmann reaction. Chem Rev 102:1359–1470
16. Negishi E, Anastasia L (2003) Palladium-catalyzed alkynylation. Chem Rev 103:1979–2017

17. Heravi MM, Sadjadi S (2009) Recent advances in the application of the Sonogashira method in the synthesis of heterocyclic compounds. Tetrahedron 65:7761–7775
18. Heravi MM, Tajbakhsh M, Ramezanian N (1998) Sulfuric acid adsorbed on silicagel: an inexpensive catalyst for regioselective cyclization of 3-propargylthio-s-triazole to 5-methylthiazolo[3,2-b]-s-triazole. Indian J Heterocycl Chem 7:309–310
19. Heravi MM, Tajbakhsh M (1998) Sodium hydroxide: a mild and inexpensive catalyst for the regioselective synthesis of 2-substituted 5-methylthiazolo[3,2-b]-s-triazoles. J. Chem. Res. 488–490
20. Heravi MM, Khademalfoghara HR, Sadeghi MM, Khaleghi Sh, Ghassemzadeh M (2006) Solvent free regioselective cyclization of 3-allylmercapto-1,2,4-triazoles to thiazolo[3,2-b]1,2,4-triazoles over sulfuric acid adsorbed on silica gel. 181:377–380
21. Becke AD (1993) A new mixing of Hartree-Fock and local density-functional theories. J Chem Phys 98:1372–1377
22. Lee C, Yang W, Parr RG (1988) Development of the Colle-Salvetti correlation-energy formula into a functional of the electron density. Phys Rev B37:785–789
23. Barone V, Cossi M (1998) Quantum calculation of molecular energies and energy gradients in solution by a conductor solvent model. J Phys Chem A102:1995–2001
24. Amatore C, Carré E, Jutand A (1998) Evidence for an equilibrium between neutral and cationic arylpalladium(II) complexes in DMF. Mechanism of the reduction of cationic arylpalladium(II) complexes. Acta Chem Scand 52:100–106
25. Truhlar DG, Zhao Y (2008) The M06 suite of density functionals for main group thermochemistry, thermochemical kinetics, noncovalent interactions, excited states, and transition elements: two new functionals and systematic testing of four M06-class functionals and 12 other functional. Theor Chem Account 120:215–241
26. Wadt WR, Hay PJ (1985) Ab initio effective core potentials for molecular calculations. Potentials for main group elements Na to Bi. J Chem Phys 82:284–298
27. Schmidt MW, Baldridge KK, Boatz JA, Elbert ST, Gordon MS, Jensen JH, Koseki S, Matsunaga N, Nguyen KA, Su SJ, Windus TL, Dupuis M, Montgomery JA (1993) General atomic and molecular electronic structure system. J Comput Chem 14:1347–1363
28. Heravi MM, Kivanloo A, Rahimzadeh M, Bakavoli M, Ghassemzadeh M (2002) Heteroannulation through palladium catalysis: a novel cyclization leading to regioselective synthesis of 3-substituted thiazolo[3,2-C]1,2,4-triazin-5-ones. Phosphorus Sulfur Silicon 177:2491–2496
29. Heravi MM, Kivanloo A, Rahimzadeh M, Bakavoli M, Ghassemzadeh M, Neumüller B (2005) Regioselective synthesis of 3-benzylthiazolo[3,2-a]pyrimidones and 3-benzyl-thiazolo[3,2-c]pyrimidones through palladium-catalyzed heteroannulation of acetylenic compounds. Phosphorus Sulfur Silicon 180:2407–2417